

MKPH-T-97-4

Coherent η -photoproduction on ^4He and ^{12}C in the near-threshold region ^{*}

A. Fix[†] and H. Arenhövel

Institut für Kernphysik, Johannes Gutenberg-Universität, D-55099 Mainz, Germany

(July 8, 2021)

Abstract

Coherent η meson photoproduction on ^4He and ^{12}C is considered in the near-threshold region. The elementary η photoproduction operator includes contributions from the $S_{11}(1535)$ and $D_{13}(1520)$ resonances as well as t -channel vector meson exchange and the nucleon pole terms. Due to the suppression of the dominant $S_{11}(1535)$ resonance for spin and isospin saturated nuclei, the reaction is mainly governed by ω exchange. Furthermore, the influence of Fermi motion and of different prescriptions for the choice of the invariant reaction energy $W_{\gamma N}$ in the elementary amplitude is studied.

PACS number(s): 13.60 Le, 25.20 Lj

Typeset using REVTeX

^{*}Supported by the Deutsche Forschungsgemeinschaft (SFB 201)

[†]Supported by the Deutscher Akademischer Austauschdienst

I. INTRODUCTION

During the past few years a large number of experimental and theoretical investigations of η meson photoproduction on nucleon and nuclei has been undertaken. Because of the isoscalar nature of the η meson, these reactions yield unique information concerning the properties of baryon resonances with isospin $T=1/2$. Most of the past theoretical work was devoted to the study of the $S_{11}(1535)$ resonance and its properties in nuclear matter [1,2,3,4,5]. This resonance has a dominant contribution in η production on the nucleon near threshold because of its strong coupling to the ηN channel. As a consequence, the observation of other resonances and of the nonresonant terms is possible only via their interference with the dominant $S_{11}(1535)$ excitation amplitude. Therefore, theoretical predictions about their properties extracted from the $\gamma N \rightarrow \eta N$ analysis depend considerably on the $S_{11}(1535)$ parameters which are not well known yet. This problem may be solved by studying η photoproduction on nuclei which can be used as spin-isospin filters allowing one to investigate the individual parts of the elementary amplitude.

In this spirit, the coherent η photoproduction on spin-isospin saturated nuclei is of special interest, because in these processes the $S_{11}(1535)$ resonance is suppressed, and thus the corresponding cross sections are sensitive to the “small” parts of the elementary photoproduction operator. On the other hand, a disadvantage of such reactions is the difficulty of their experimental isolation due to the smallness of the coherent cross section compared to the background quasifree process $A(\gamma, \eta)$. As a consequence, rather little effort has been devoted to their theoretical study. This situation will probably change in the near future with new measurements of η photoproduction on nuclei with c.w. electron machines, like for example, on ${}^4\text{He}$ with MAMI [6]. In anticipation of such experiments, we present here theoretical results for η photoproduction on spin-isospin saturated nuclei, for which we have chosen as specific examples ${}^4\text{He}$ and ${}^{12}\text{C}$.

An early, rather detailed study of these processes was performed by Bennhold and Tanabe [7]. Their elementary model, based on a coupled channel approach, gave a satisfactory

description of the at that time available data on the $\gamma p \rightarrow \eta p$ reaction, which, however, were not very precise. Their approach is a pure isobar model and does not include any background terms. On the other hand, such terms *a priori* give nonnegligible contributions to the elementary amplitude and their role in coherent reactions may be important. Therefore, with the appearance of new precise $\gamma p \rightarrow \eta p$ data [1] it is interesting to review the theoretical results for η photoproduction on such nuclei by including such background terms.

Our treatment of the elementary process follows the effective Lagrangian approach used for the analysis of meson photoproduction by many authors [2,4,8]. The $\gamma N \rightarrow \eta N$ amplitude is obtained by means of second-order Feynman diagrams for the nucleon pole and vector mesons exchange as well as for the resonant states which are expected to give significant contributions to η photoproduction in the near-threshold region. The advantage of this approach is that it gives a production operator valid for an arbitrary frame in a rather simple analytical form which is convenient for the implementation into the nuclear (γ, η) process. The ingredients of the model are presented in Sect. 2. In Sect. 3 we discuss our results for the coherent reactions on ${}^4\text{He}$ and ${}^{12}\text{C}$, and compare them with those obtained by other authors. Conclusions are given in Sect. 4.

II. THE ELEMENTARY PROCESS

The details of the kinematics and the structure of the η photoproduction amplitude on the nucleon have been described in [2,4,7]. Therefore, we give in this section only a brief summary of the elementary reaction

$$\gamma(k_\mu, \vec{\varepsilon}_\lambda) + N(p_\mu) \rightarrow \eta(q_\mu) + N(p'_\mu), \quad (1)$$

in order to establish the notation and to describe the ingredients. Throughout the paper, the conventions of Bjorken and Drell [9] are used. The four-momenta of the participating particles are denoted by

$$k_\mu = (k_0, \vec{k}), \quad q_\mu = (q_0, \vec{q}), \quad p_\mu = (p_0, \vec{p}), \quad p'_\mu = (p'_0, \vec{p}'), \quad (2)$$

for photon, η meson, initial and final nucleon, respectively, and the photon polarization vector by $\vec{\varepsilon}_\lambda$. The particle energies are

$$k_0 = k, \quad q_0 = \sqrt{q^2 + m_\eta^2}, \quad p_0^{(\prime)} = \sqrt{p^{(\prime)2} + m^2}, \quad (3)$$

where m and m_η stand for the masses of nucleon and η meson, and k , q , p , and p' denote the absolute values of the respective three-momenta.

The S -matrix of the process (1) is given by

$$S_{fi} = \delta_{fi} - i(2\pi)^4 \delta^4(p'_\mu + q_\mu - p_\mu - k_\mu) \sqrt{\frac{m^2}{2k_0 2q_0 p_0 p'_0}} T_{fi}, \quad (4)$$

where the transition matrix element T_{fi} can be written in terms of CGLN amplitudes [10]

$$T_{fi} = T_{s's\lambda} = \bar{u}_f(p', s') \left[\sum_{j=1}^4 A_j(s, t, u) M_{j\lambda} \right] u_i(p, s). \quad (5)$$

Here, $u_i(p, s)$ and $u_f(p', s')$ denote the covariantly normalized Dirac spinors of the intial and final nucleon, respectively, $M_{j\lambda}$ the gauge invariant CGLN operators and A_j the invariant scalar amplitudes which depend on the Mandelstam variables

$$s = (k_\mu + p_\mu)^2, \quad t = (k_\mu - q_\mu)^2, \quad u = (k_\mu - p'_\mu)^2. \quad (6)$$

The polarization averaged $\gamma N \rightarrow \eta N$ differential cross section in the γN c.m. system is related to the T -matrix (5) by

$$\frac{d\sigma}{d\Omega^{c.m.}} = \frac{1}{(4\pi)^2} \frac{q}{k} \frac{m^2}{W_{\gamma N}^2} \frac{1}{4} \sum_{s's\lambda} |T_{s's\lambda}|^2, \quad (7)$$

where $W_{\gamma N} = \sqrt{s}$ is the γN invariant mass.

Fig. 1 shows the Feynman diagrams included in our calculation. The corresponding vertex functions and propagators are listed in Tables I and II. For the ηNN vertex we use pseudoscalar coupling with $g_{\eta NN}^2/4\pi=0.4$ in agreement with [11,12] in the analysis of experimental $\gamma p \rightarrow \eta p$ angular distributions [1]. All parameters for the vector meson t -channel exchange with ρ and ω mesons are given in Table III. We use the empirical hadronic coupling constants from the compilation of Dumbrajs *et al.* [13]. The radiative couplings λ_V

$(V = \rho, \omega)$ may be extracted from the electromagnetic decay widths $\Gamma(V \rightarrow \gamma\eta)$ [14,15] and were determined in Ref. [2]. A monopole form factor,

$$F(t) = \frac{\Lambda_V^2 - m_V^2}{\Lambda_V^2 - t}, \quad (8)$$

with $\Lambda_V^2 = 2m_V^2$ has been introduced at the VNN vertices.

The resonance part of the amplitude is represented by two $T = 1/2$ resonances - $S_{11}(1535)$ and $D_{13}(1520)$ - which contribute significantly to η photoproduction in the near-threshold region. The other resonances can be neglected because of their large masses and/or small couplings to the ηN channel [2]. Also the Roper resonance $P_{11}(1440)$ is omitted in our calculation because it is below the ηN threshold and its coupling to this channel is not well determined. The analysis of the new Mainz data [1] indicates anyway a small role of this resonance in η production [2]. The relevant resonance parameters are listed in Table III. The mass and width as well as the helicity couplings for the $D_{13}(1520)$ were taken from the 1996 PDG listings [15]. The corresponding values for the dominant $S_{11}(1535)$ resonance were considered as adjustable parameters in fitting the new data on the total $\gamma p \rightarrow \eta p$ cross section [1]. The ratio $A_{1/2}^n/A_{1/2}^p$ of the neutron to the proton amplitude of the $S_{11}(1535)$ photoexcitation was taken from Ref. [16] as obtained from the analysis of the inclusive $d(\gamma, \eta)$ cross section, where the rescattering effects in the final state were taken into account. Furthermore, for $S_{11}(1535)$ we use an energy dependent decay width

$$\Gamma(W_{\gamma N}) = \Gamma(M_{S_{11}}) \left(b_\eta \frac{q}{q^*} + b_\pi \frac{q_\pi}{q_\pi^*} + b_{\pi\pi} \right), \quad (9)$$

with the branching ratios $b_\eta = 0.5$, $b_\pi = 0.4$ and $b_{\pi\pi} = 0.1$. Here q and q_π are the η and π meson momenta in the γN c.m. system as functions of $W_{\gamma N}$, and q^* and q_π^* are the respective momenta at $W_{\gamma N} = M_{S_{11}}$.

With respect to the $D_{13}(1520)$ resonance, it is known that the relativistic treatment of a $J = 3/2$ particle contains an ambiguity related to its off-mass-shell extrapolation [17]. As a consequence, the implementation of the free Rarita-Schwinger propagator in the intermediate off-mass-shell state leads to the appearance of a resonance contribution in the nonresonant

amplitudes. In order to avoid this ambiguity, following Ref. [18], we have replaced the resonance mass $M_{D_{13}}$ in the numerator of the $D_{13}(1520)$ propagator by the invariant energy $W_{\gamma N}$ (see Table II). Furthermore, we have omitted the $D_{13}(1520)$ formation in the u channel, where the resonance is always far off-shell. We will also consider medium modifications of the width when implementing the elementary amplitude in a nucleus as will be discussed in Sect. 3.

The invariant amplitudes A_i , corresponding to the individual terms in Fig. 1, are collected in the Appendix. In Fig. 2 the predictions of our elementary model for the $\gamma p \rightarrow \eta p$ differential cross section are compared with new Mainz data [1]. One readily notes that a satisfactory agreement is achieved. We would like to point out that within our parametrization the contributions from nucleon pole and vector meson exchange cancel each other almost completely, leaving practically the whole angular distribution to be given by the $S_{11}(1535)$ and $D_{13}(1520)$ resonances.

For the calculation of η photoproduction on a nucleus with nonrelativistic wave functions, it is necessary to express the photoproduction amplitude in terms of Pauli matrices and two-component spinors. Therefore, we introduce a corresponding t -operator by

$$\chi_{s'}^\dagger t_\lambda \chi_s = \bar{u}_f(p', s') \left[\sum_j A_j M_{j\lambda} \right] u_i(p, s), \quad (10)$$

and decompose it into a so-called non-spin-flip and a spin-flip part according to

$$t_\lambda = K(\vec{\varepsilon}_\lambda) + i \vec{L}(\vec{\varepsilon}_\lambda) \cdot \vec{\sigma}. \quad (11)$$

The amplitudes K and \vec{L} can be written in the following form

$$\begin{aligned} K(\vec{p}', \vec{p}, \vec{k}, \vec{\varepsilon}) &= F_1 \left(\frac{\vec{p} \cdot (\vec{\varepsilon} \times \vec{k})}{p_0 + m} - \frac{\vec{p}' \cdot (\vec{\varepsilon} \times \vec{k})}{p'_0 + m} \right) \\ &+ F_2 \frac{\vec{p}' \cdot (\vec{\varepsilon} \times \vec{p})}{(p_0 + m)(p'_0 + m)} + F_3 \frac{\vec{p}' \cdot (\vec{k} \times \vec{p})}{(p_0 + m)(p'_0 + m)}, \end{aligned} \quad (12)$$

$$\vec{L}(\vec{p}', \vec{p}, \vec{k}, \vec{\varepsilon}) = \vec{\varepsilon} \left[F_1 \left(2k_0 - \frac{\vec{k} \cdot \vec{p}}{p_0 + m} - \frac{\vec{k} \cdot \vec{p}'}{p'_0 + m} \right) + F_2 \left(\frac{\vec{p} \cdot \vec{p}'}{(p_0 + m)(p'_0 + m)} - 1 \right) \right]$$

$$\begin{aligned}
& + \vec{k} \left[F_1 \left(\frac{\vec{\varepsilon} \cdot \vec{p}}{p_0 + m} + \frac{\vec{\varepsilon} \cdot \vec{p}'}{p'_0 + m} \right) + F_3 \left(\frac{\vec{p} \cdot \vec{p}'}{(p_0 + m)(p'_0 + m)} - 1 \right) \right] \\
& + \vec{p} \left[\frac{F_4}{p_0 + m} - F_2 \frac{\vec{\varepsilon} \cdot \vec{p}'}{(p_0 + m)(p'_0 + m)} - F_3 \frac{\vec{k} \cdot \vec{p}'}{(p_0 + m)(p'_0 + m)} \right] \\
& + \vec{p}' \left[\frac{F_4 + 2k_0 F_3}{p'_0 + m} - F_2 \frac{\vec{\varepsilon} \cdot \vec{p}}{(p_0 + m)(p'_0 + m)} - F_3 \frac{\vec{k} \cdot \vec{p}}{(p_0 + m)(p'_0 + m)} \right] \quad (13)
\end{aligned}$$

where $\vec{p}' = \vec{p} + \vec{k} - \vec{q}$, and $\vec{\varepsilon}$ denotes the photon polarization vector. Furthermore, the F_i are expressed in terms of A_i as follows

$$F_1 = N' N (A_1 - 2mA_4), \quad (14)$$

$$F_2 = N' N \left[k_0 (A_1 - 2mA_4) + A_3 k^\mu (p'_\mu - p_\mu) - A_4 k^\mu (p'_\mu + p_\mu) \right], \quad (15)$$

$$F_3 = N' N \left[A_3 \vec{\varepsilon} \cdot (\vec{p}' - \vec{p}) - A_4 \vec{\varepsilon} \cdot (\vec{p}' + \vec{p}) \right], \quad (16)$$

$$F_4 = N' N \left[2A_2 (\vec{\varepsilon} \cdot \vec{p}' k^\mu p_\mu - \vec{\varepsilon} \cdot \vec{p} k^\mu p'_\mu) - k_0 A_3 \vec{\varepsilon} \cdot (\vec{p} - \vec{p}') - k_0 A_4 \vec{\varepsilon} \cdot (\vec{p} + \vec{p}') \right], \quad (17)$$

with $N = \sqrt{(p_0 + m)/2m}$, $N' = \sqrt{(p'_0 + m)/2m}$.

When applying the elementary operator (11)-(13) to a bound nucleon, which is always off-mass-shell, the energies p_0 and p'_0 are not defined in a nonrelativistic framework, and thus the problem of assigning an energy to a bound nucleon arises. This question will be addressed in the next section.

The spin-dependent amplitude \vec{L} , which is dominated by the $S_{11}(1535)$ excitation, plays a major role in η photoproduction on a free nucleon. However, due to the spin-isospin selection rules, the coherent (γ, η) process on $J = T = 0$ nuclei is essentially determined by the isoscalar part of the non-spin-flip amplitude $K^{(0)}$. Therefore, the influence of the $S_{11}(1535)$ resonance is largely suppressed in this case. It should be noted, however, that by the spin decomposition of the elementary operator in the ηN c.m. system, the contribution from $S_{11}(1535)$, which determines the electric dipole amplitude E_{0+} , enters only into the spin-dependent component \vec{L} . But in general for an arbitrary frame, a small contribution from this resonance is mixed into the spin-independent part K . Although this mixing normally is insignificant relative to the \vec{L} -term, the resulting effect may be noticeable if the spin-flip term is suppressed, because of the relatively large strength of the $S_{11}(1535)$ contribution in

the $\gamma N \rightarrow \eta N$ amplitude.

III. COHERENT η PHOTOPRODUCTION ON NUCLEI

Now we will consider the near-threshold coherent η photoproduction on a nucleus

$$\gamma + A \rightarrow \eta + A \quad (18)$$

with mass number A , spin $J=0$ and isospin $T=0$. In this case, the differential cross section in the γ -nucleus c.m. frame can be written as

$$\frac{d\sigma}{d\Omega^{c.m.}} = \frac{1}{(4\pi)^2} \frac{q}{k} \frac{E_{A,k} E_{A,q}}{W_{\gamma A}^2} \frac{1}{2} \sum_{\lambda} |T_{A,\lambda}^{c.m.}(\vec{k}, \vec{q})|^2, \quad (19)$$

where $W_{\gamma A}$ denotes the invariant mass of the γA system and $E_{A,k}$ and $E_{A,q}$ the initial and final nuclear energies, respectively, i.e., $E_{A,p} = \sqrt{p^2 + M_A^2}$ with the nuclear mass M_A . The nuclear states are noncovariantly normalized to unity. In the laboratory frame the cross section is given by

$$\frac{d\sigma}{d\Omega^{lab}} = \frac{1}{(4\pi)^2} \frac{q_L^2}{k_L} \frac{E_{A,q_L}}{q_L(M_A + k_L) - k_L E_{q_L} \cos \theta_L} \frac{1}{2} \sum_{\lambda} |T_{A,\lambda}^{lab}(\vec{k}_L, \vec{q}_L)|^2, \quad (20)$$

where all quantities refer to the laboratory frame. In order to check the frame independence of the calculation, we will compare the direct evaluation of (19) with the calculation obtained in the lab frame from (20) and subsequently transformed with the Jacobian

$$\frac{d\Omega^{lab}}{d\Omega^{c.m.}} = \frac{q^2}{q_L} \frac{M_A}{E_{A,k} q + E_q k \cos \theta} \quad (21)$$

to the c.m. frame.

In the impulse approximation (IA), the nuclear photoproduction amplitude is given as a sum over the elementary amplitudes of all nucleons in the nucleus. For example, in the c.m. frame, the transition matrix $T_{A,\lambda}^{c.m.}$ can be represented in the form

$$T_{A,\lambda}^{c.m.}(\vec{k}, \vec{q}) = A \int d^3 p d^3 q' \chi_{\vec{q}}^{(-)*}(\vec{q}') K^{(0)}(\vec{p} - \frac{\vec{k}}{A} + \vec{Q}', \vec{p} - \frac{\vec{k}}{A}, \vec{k}, \vec{\varepsilon}_{\lambda}) \rho_A(\vec{p} + \vec{Q}', \vec{p}), \quad (22)$$

where $\vec{Q}' = \vec{k} - \vec{q}'$. Here $\rho_A(\vec{p}', \vec{p})$ denotes the one-body nuclear density matrix of the nuclear ground state in momentum space

$$\rho_A(\vec{p}', \vec{p}) = \langle A | a^\dagger(\vec{p}') a(\vec{p}) | A \rangle, \quad (23)$$

where $a^\dagger(\vec{p})$ and $a(\vec{p})$ denote creation and annihilation operators for a bound nucleon with momentum \vec{p} in the nuclear rest frame. The isoscalar part $K^{(0)}$ of the spin-independent amplitude (12) is defined as $K^{(0)} = 1/2(K_p + K_n)$ with index p referring to the proton and n to the neutron. The function $\chi_{\vec{q}}^{(-)}(\vec{q}')$ describes the relative motion of the outgoing η with respect to the recoiling nucleus including a final state interaction via an optical potential. Since we are interested in the main properties of the reaction (18), we simplify further and ignore here the η -nucleus interaction. This means, we substitute $\chi_{\vec{q}}^{(-)}(\vec{q}')$ by the free meson function $\delta(\vec{q} - \vec{q}')$ in the matrix element (22) leading with (23) to

$$T_{A,\lambda}^{c.m.}(\vec{k}, \vec{q}) = A \int d^3p K^{(0)}(\vec{p} - \frac{\vec{k}}{A} + \vec{Q}, \vec{p} - \frac{\vec{k}}{A}, \vec{k}, \vec{\varepsilon}_\lambda) \rho_A(\vec{p} + \vec{Q}, \vec{p}), \quad (24)$$

where $\vec{Q} = \vec{k} - \vec{q}$ is the transferred momentum.

In order to avoid the complication of the nuclear Fermi motion in the evaluation of (24), a further approximation is widely used in the study of meson photoproduction on light nuclei [7,20] which allows one to express the matrix element in terms of the nuclear body form factor $F_A(Q)$. It is the so-called factorization approximation [7] which we give here with respect to the laboratory frame for convenience

$$T_{A,\lambda}^{lab}(\vec{k}_L, \vec{q}_L) = A F_A(Q_L) K^{(0)}(\vec{p}_{eff} + \vec{Q}_L, \vec{p}_{eff}, \vec{k}_L, \vec{\varepsilon}_\lambda), \quad (25)$$

where the elementary operator is frozen at the average effective nucleon momentum in the nuclear rest system, i.e., the lab system

$$\vec{p}_{eff} = -\frac{A-1}{2A} \vec{Q}_L, \quad (26)$$

which corresponds to the following assignments in the γA c.m. frame [20]

$$\vec{p} = -\frac{1}{A} \vec{k} - \frac{A-1}{2A} \vec{Q}, \quad (27)$$

$$\vec{p}' = -\frac{1}{A} \vec{q} + \frac{A-1}{2A} \vec{Q}. \quad (28)$$

In this approximation, the nucleon energies p_0 and p'_0 are taken on shell. The exact treatment of the Fermi motion by a direct computation of the three-dimensional integral in the matrix element of (24) will be discussed below for ${}^4\text{He}$.

For ${}^{12}\text{C}$ we have taken a phenomenological fit for the charge form factor $F_{{}^{12}\text{C}}^{ch}(Q)$ from [19]

$$F_{{}^{12}\text{C}}^{ch}(Q) = -\frac{3\pi b [\cos(QR) - (\pi b/R) \sin(QR) \coth(\pi bQ)]}{QR^2 \sinh(\pi bQ)[1 + \pi^2 b^2/R^2]}, \quad (29)$$

with two parameters $R = 2.179$ fm and $b = 0.503$ fm. The body form factor is then obtained by

$$F_{{}^{12}\text{C}}(Q) = [F_p(Q)]^{-1} F_{{}^{12}\text{C}}^{ch}(Q), \quad (30)$$

with the proton form factor $F_p(Q)$ taken in the dipole parametrization

$$F_p(Q) = \frac{1}{(1 + 0.055(Q/\text{fm}^{-1})^2)^2}. \quad (31)$$

For ${}^4\text{He}$ we use as wave function a product ansatz which consists of a relative motion of the active nucleon with respect to the spectator nucleons building a $3N$ cluster with an internal wave function. The relative motion is described by an s -wave $\psi(\vec{r})$ with \vec{r} being the relative coordinate in the $N - (3N)$ system. The internal cluster wave function is not needed since we neglect antisymmetrization between the active nucleon and the $3N$ -cluster. For $\psi(\vec{r})$ we have taken from [21] the phenomenological form

$$\psi(r) = N \frac{e^{-\alpha r}}{r} \sum_{j=1}^5 a_j e^{-\beta_j r}, \quad (32)$$

where $\alpha = 0.846 \text{ fm}^{-1}$ and the parameters a_j and β_j are listed in Table IV. The corresponding body form factor, which can be written as

$$F_{{}^4\text{He}}(Q) = \int d^3r |\psi(r)|^2 e^{i\frac{3}{4}\vec{Q}\cdot\vec{r}} = 4\pi N^2 \frac{4}{3Q} \sum_{ij} a_i a_j \arctan \frac{3Q}{4(2\alpha + \beta_i + \beta_j)}, \quad (33)$$

fits the measured ${}^4\text{He}$ charge form factor up to its second maximum. The functional form (32) allows also a simple analytic expression for the momentum space representation

$$\psi(p) = \int d^3r \psi(r) e^{i\frac{3}{4}\vec{p}\cdot\vec{r}} = 4\pi N \sum_j \frac{a_j}{(\alpha + \beta_j)^2 + (3p/4)^2}, \quad (34)$$

which is needed for the explicit evaluation of the Fermi motion in the integral of (24).

We begin the discussion of our results with the total cross sections for the coherent reactions ${}^4\text{He}(\gamma, \eta){}^4\text{He}$ and ${}^{12}\text{C}(\gamma, \eta){}^{12}\text{C}$ which are shown in Fig. 3. One readily notes that the coherent cross section on $J = T = 0$ nuclei is very small in magnitude, of the relative order of 10^{-3} , compared to the incoherent process (see for example [23]). This is mainly due to the suppression of the in the elementary reaction dominant $S_{11}(1535)$ resonance. Another reason is that the coherent nuclear transition amplitude via the body form factor falls off rapidly at the high momentum transfers associated with the η production. Although the coherence factor A^2 is nine times bigger for ${}^{12}\text{C}$ compared to ${}^4\text{He}$, the cross section for ${}^{12}\text{C}$ is considerably smaller because of the much faster fall-off of the body form factor with momentum transfer Q .

The contributions of the individual terms of our elementary $\gamma N \rightarrow \eta N$ model are illustrated in Fig. 4 for the differential cross section of ${}^{12}\text{C}$. As mentioned before, the $S_{11}(1535)$ resonance has some influence on the non-spin-flip part of the elementary operator. But as one can see on the right hand panel of Fig. 4, this effect remains negligible, since the isoscalar part of the $S_{11}(1535)$ amplitude, used in our calculation, is rather small ($T^{(0)}/T_p = 0.076$). It is obvious that of the vector mesons only the isoscalar ω meson contributes to the amplitude here. In fact, one can see on the left hand panel of Fig. 4 that this term dominates the nuclear cross section, while the isoscalar part of the nucleon pole terms gives also an insignificant contribution.

As for the $D_{13}(1520)$ resonance, we have taken into account a possible modification of its properties in a nuclear environment. Experimental results on total photoabsorption [22] as well as π^0 photoproduction on light nuclei [23] show a strong depletion of the resonance structure in the region of the $D_{13}(1520)$ resonance. This effect may be attributed to a strong shortening of the $D_{13}(1520)$ lifetime in a nucleus, where additional absorption channels, involving inelastic NN^* collisions, increase the resonance width. We have simulated such

effects in our calculations by simply replacing the free resonance width by an effective one, i.e., $\Gamma \rightarrow \Gamma^*$. The value $\Gamma^* = 265$ MeV for the $D_{13}(1520)$ was obtained in Ref. [24] from the analysis of total photoabsorption on ^9Be and ^{12}C . A questionable point of this treatment is that the parameters, extracted from ^9Be and ^{12}C data, may not be appropriate for such a light nucleus like ^4He . However, we believe that the possible error is not dramatic and does not lead to a qualitative change of the results. This medium modification of the $D_{13}(1520)$ width leads to a noticeable damping of its contribution to the cross section, as is demonstrated in the right hand panel of Fig. 4. In summary, our calculation shows a clear dominance of ω exchange in the coherent cross section for spin-isospin saturated nuclei, while the role of the nucleon pole terms as well as of the resonances is not important.

Another remark about the role of the $D_{13}(1520)$ resonance is concerned with the fact, that ω exchange contributes to the real part of the η production amplitude only, while the real part of the amplitude of the $D_{13}(1520)$, located near the η production threshold, is relatively small. For this reason, we find very little interference between these amplitudes in the nuclear cross section. This is in marked contrast to a very recent result of [25] where a strong constructive interference between vector meson exchange and $D_{13}(1520)$ excitation increases the cross section of the coherent reaction on ^{40}Ca substantially. The reason is not clear to us.

Now we turn to the discussion of the exact treatment of the nuclear Fermi motion. In the explicit evaluation of the integral in (24), one faces the problem of fixing the invariant mass of the γN subsystem

$$W_{\gamma N} = \sqrt{(k_0 + p_0)^2 - (\vec{k} + \vec{p})^2}. \quad (35)$$

In fact, this question is connected with the choice of the energy of the active bound nucleon in the off-shell region, where $p_0^2 \neq m^2 + p^2$. The analogous problem for the coherent process on the deuteron has already been discussed in Ref. [4]. There it was shown that various prescriptions for $W_{\gamma N}$ lead to significantly different results. It should be noted, however, that the η photoproduction on the deuteron is dominated by the $S_{11}(1535)$ resonance, and

thus the corresponding amplitude depends directly on $W_{\gamma N}$ appearing in the resonance propagator. In addition, the choice of $W_{\gamma N}$ has a large influence on the width $\Gamma_{S_{11}}(W_{\gamma N})$ to which the cross section is also very sensitive.

On the other hand, in view of the dominant t -channel ω exchange for the coherent (γ, η) processes considered here, one would expect that the cross section will be rather insensitive to the different assumptions on $W_{\gamma N}$. In order to investigate this question, we have considered for the ${}^4\text{He}(\gamma, \eta){}^4\text{He}$ reaction the following alternative prescriptions for $W_{\gamma N}$ in the $\gamma {}^4\text{He}$ c.m. system:

$$W_{\gamma N}^{(1)} = \left[\frac{1}{E_{A,k}^2} \left(\frac{M_A^2}{4} + k_0 E_{A,k} - \vec{k} \cdot \vec{p} \right)^2 - (\vec{k} + \vec{p})^2 \right]^{1/2}, \quad (36)$$

$$W_{\gamma N}^{(2)} = \left[(k_0 + \sqrt{p^2 + m^2})^2 - (\vec{k} + \vec{p})^2 \right]^{1/2}, \quad (37)$$

where $E_{A,k}$ is the ${}^4\text{He}$ c.m. energy in the initial state. The first choice (36) corresponds to the assumption, that all nucleons share equally the total energy of ${}^4\text{He}$ in its rest system

$$p_0^{lab} = \frac{M_A}{4}. \quad (38)$$

In the second expression (37), the active nucleon is taken on-shell before the production process. This case has also been considered in Ref. [26] for the ${}^3\text{He}(\gamma, \pi^+) {}^3\text{H}$ reaction. Our results, corresponding to the different choices of $W_{\gamma N}$ are shown in Fig. 5. The only term, which can be significantly affected by the value of $W_{\gamma N}$ and which can have some noticeable influence on the cross section, is the $D_{13}(1520)$ excitation term in our model. We note that in the whole region of nucleon momentum \vec{p} one has the relation

$$W_{\gamma N}^{(1)} < W_{\gamma N}^{(2)}, \quad (39)$$

because the binding energy of the nucleon, which is taken into account in (36), decreases its total energy. Thus the different choices for $W_{\gamma N}$ lead to different results for the magnitude and position of the $D_{13}(1520)$ resonance in the nuclear cross section. However, since the resonance contribution is small, the influence of this uncertainty in $W_{\gamma N}$ is not significant as can be seen in Fig. 5.

In this figure we also display the ${}^4\text{He}(\gamma, \eta){}^4\text{He}$ angular distribution obtained within the factorization approximation (25), where the elementary amplitude is taken on-shell. The rather small difference between the corresponding curves shows, that the exact treatment of Fermi motion differs little from the factorization approach which might not be so surprising after all, because of the dominance of ω exchange. Therefore, we use this approximation in the following calculations.

The study of η photoproduction on the free nucleon indicates, that the role of ω exchange in this reaction is relatively small, because of the small radiative coupling λ_ω to the $\gamma\eta$ -channel. As a result, the elementary cross section is rather insensitive to the uncertainties in the ω parameters. However, from our analysis of the coherent (γ, η) process on $J = T = 0$ nuclei, where the ω exchange dominates, it is expected that these uncertainties will be reflected in the nuclear cross section. We therefore have also investigated the sensitivity of the ${}^4\text{He}(\gamma, \eta){}^4\text{He}$ reaction to the choice of the vector coupling constant $g_{\omega NN}^v$ for which one finds a significant variation of values in the literature [13]. In our calculation we have used $g_{\omega NN}^v = 10.3$ which is close to the quark model prediction $g_{\omega NN}^v \approx 11.5$ [27]. On the other hand, in Ref. [28] a value $g_{\omega NN}^v = 17.5$ has been chosen in order to reproduce the near-threshold $\gamma p \rightarrow \pi^0 p$ data. The resulting cross section using this value of $g_{\omega NN}^v$ is shown in Fig. 6. As one can see, with the larger coupling constant the cross section increases by about a factor of 3, which is roughly the square of the ratio of the coupling constants. In principle, this high sensitivity to the ω exchange makes it possible to determine the value of the ωNN coupling constant by a precise measurement of coherent η photoproduction on $J = T = 0$ nuclei provided that neglected two-body effects are small indeed.

We have furthermore checked the frame independence of the calculation by comparing the c.m. differential cross section obtained directly in the c.m. frame with the one evaluated first in the lab frame according to (20) and then transformed with the help of the Jacobian (21) to the c.m. frame. The resulting cross sections are shown in Fig. 7 for ${}^4\text{He}$. Indeed, the differences are very small indicating that c.m. motion effects are insignificant. We have checked it also for ${}^{12}\text{C}$ where the differences are completely negligible.

Finally, we compare in Fig. 8 our results for ${}^4\text{He}(\gamma, \eta){}^4\text{He}$ with those obtained by other authors. As has been mentioned before, the coherent reactions, considered here, were already investigated in Ref. [7], where the elementary amplitude was obtained in the framework of a coupled channel approach. In this work, the isoscalar $M_{2-}^{(0)}$ multipole from the $D_{13}(1520)$ resonance plays a dominant role in ${}^4\text{He}(\gamma, \eta){}^4\text{He}$ reaction, while the nonresonant terms were omitted. This is quite contrary to our conclusion, that ω exchange gives the major mechanism of coherent (γ, η) processes on $J = T = 0$ nuclei. Therefore, the cross section from [7] is by a factor 6 larger than our result, as can be seen in the left hand panel of Fig. 8. Recently, another evaluation of η photoproduction on ${}^4\text{He}$ in the PWIA approximation has been presented in [11] using the model of [7], but with inclusion of the background terms considered in the present work. In order to compare the results, we have calculated ${}^4\text{He}(\gamma, \eta){}^4\text{He}$ cross section with the same parameters in the t -channel as in Ref. [11]. The corresponding cross section, shown in the right hand panel of Fig. 8, underestimates still the one of [11] by about 30 percent.

In order to explain the origin of these differences, we compare in Fig. 9 the isoscalar part of the CGLN amplitude \mathcal{F}_2 as predicted in [7] with our model. This amplitude, appearing in the usual form for the photoproduction operator

$$F = i\mathcal{F}_1\vec{\sigma} \cdot \vec{\varepsilon} + \mathcal{F}_2\vec{\sigma} \cdot \hat{q}\vec{\sigma} \cdot (\hat{k} \times \vec{\varepsilon}) + i\mathcal{F}_3\vec{\sigma} \cdot \hat{k}\hat{q} \cdot \vec{\varepsilon} + i\mathcal{F}_4\vec{\sigma} \cdot \hat{k}\hat{q} \cdot \vec{\varepsilon}, \quad (40)$$

plays a major role in the coherent meson photoproduction on $J = T = 0$ nuclei. As one readily notes in Fig. 9, the value of $\mathcal{F}_2^{(0)}$ as given by our calculation is significantly smaller than the one of Ref. [7] in the near-threshold region. As already mentioned, in [7] the latter is dominated by the resonant $M_{2-}^{(0)}$ multipole which is much larger in comparison with our one. Furthermore, as was discussed above, we have taken into account the broadening of the $D_{13}(1520)$ resonance in a nuclear environment, reducing further its contribution to (γ, η) reactions.

IV. CONCLUSION

We have studied coherent η photoproduction from the spin-isospin saturated nuclei ${}^4\text{He}$ and ${}^{12}\text{C}$. The elementary production operator was obtained in the effective Lagrangian approach. Two resonances, $S_{11}(1535)$ and $D_{13}(1520)$, as well as nucleon pole terms and vector meson exchange in the t -channel were included. One main point of this work was to investigate the influence of these different contributions on the coherent (γ, η) reaction on nuclei with zero spin and isospin, where the dominant contribution from the $S_{11}(1535)$ resonance is suppressed.

Our calculations show that the reaction is dominated by the ω exchange in the t -channel, while the role of the $D_{13}(1520)$ resonance and other terms is rather small. Such “nonresonant” character leads to some peculiarities of the nuclear cross section. For example, we see little sensitivity of the theoretical results to the different assumptions about the invariant mass of the γN subsystem in the off-shell region. Furthermore, it was found that the influence of the Fermi motion on the cross section may successfully be simulated by the factorization procedure, using an effective nucleon momentum for the on-shell elementary amplitude.

Finally, we would like to emphasize again the dominant role of the ω exchange in the nuclear reaction amplitude. This is in contrast to its small contribution to the $\gamma p \rightarrow \eta p$ reaction. For this reason, its influence is rather difficult to determine in the elementary process, whereas precise experimental data on coherent (γ, η) reactions on $J = T = 0$ nuclei may allow a much cleaner study of the ω contribution.

ACKNOWLEDGMENTS

We would like to thank J. Friedrich for very useful discussions concerning various parametrizations of nuclear charge form factors. A. F. thanks R. Schmidt, M. Schwamb and P. Wilhelm for fruitful discussions.

APPENDIX: INVARIANT AMPLITUDES FOR THE REACTION $\gamma N \rightarrow \eta N$

Using the expressions for propagators and vertex factors given in Table I, the various contributions to the invariant amplitudes of (5) are as follows:

i) Nucleon pole

$$A_1 = ee_N g_{\eta NN} \left(\frac{1}{s - m^2} + \frac{1}{u - m^2} \right), \quad (\text{A.1})$$

$$A_2 = 2ee_N g_{\eta NN} \frac{1}{(s - m^2)(u - m^2)}, \quad (\text{A.2})$$

$$A_3 = -eg_{\eta NN} \frac{\kappa_N}{2m} \left(\frac{1}{s - m^2} - \frac{1}{u - m^2} \right), \quad (\text{A.3})$$

$$A_4 = -eg_{\eta NN} \frac{\kappa_N}{2m} \left(\frac{1}{s - m^2} + \frac{1}{u - m^2} \right). \quad (\text{A.4})$$

(ii) Vector meson exchange

$$A_1 = \frac{e\lambda_V}{m_\eta} \frac{g_{VNN}^t}{2m} \frac{t}{t - m_V^2}, \quad (\text{A.5})$$

$$A_2 = -\frac{e\lambda_V}{m_\eta} \frac{g_{VNN}^t}{2m} \frac{1}{t - m_V^2}, \quad (\text{A.6})$$

$$A_3 = 0, \quad (\text{A.7})$$

$$A_4 = -\frac{e\lambda_V}{m_\eta} \frac{g_{VNN}^v}{2m} \frac{1}{t - m_V^2}. \quad (\text{A.8})$$

(iii) $S_{11}(1535)$ resonance

$$A_1 = e \frac{g_{\eta NS_{11}} g_{\gamma \eta S_{11}}}{m + M_{S_{11}}} (m + M_{S_{11}}) \left(\frac{1}{s - M_{S_{11}}^2 + i\Gamma_{S_{11}} M_{S_{11}}} + \frac{1}{u - M_{S_{11}}^2} \right), \quad (\text{A.9})$$

$$A_2 = 0, \quad (\text{A.10})$$

$$A_3 = e \frac{g_{\eta NS_{11}} g_{\gamma \eta S_{11}}}{m + M_{S_{11}}} \left(\frac{1}{s - M_{S_{11}}^2 + i\Gamma_{S_{11}} M_{S_{11}}} - \frac{1}{u - M_{S_{11}}^2} \right), \quad (\text{A.11})$$

$$A_4 = e \frac{g_{\eta NS_{11}} g_{\gamma \eta S_{11}}}{m + M_{S_{11}}} \left(\frac{1}{s - M_{S_{11}}^2 + i\Gamma_{S_{11}} M_{S_{11}}} + \frac{1}{u - M_{S_{11}}^2} \right). \quad (\text{A.12})$$

(iv) $D_{13}(1520)$ resonance

$$A_1 = \frac{eg_{\eta ND_{13}}}{s - M_{D_{13}}^2 + i\Gamma M_{D_{13}}} \left[\frac{g_{\gamma ND_{13}}^{(1)}}{12mm_\eta} \left(3t - m_\eta^2 - \frac{(\sqrt{s} - m)^2}{s} (m^2 - m_\eta^2 + m\sqrt{s}) \right) \right. \\ \left. + \frac{g_{\gamma ND_{13}}^{(2)}}{48m^2m_\eta} \left(2m(3t - 2m_\eta^2) - \frac{(s - m^2)^2}{\sqrt{s}} + \frac{s + m^2}{\sqrt{s}} m_\eta^2 \right) \right], \quad (\text{A.13})$$

$$A_2 = -\frac{eg_{\eta ND_{13}}}{s - M_{D_{13}}^2 + i\Gamma M_{D_{13}}} \left[\frac{g_{\gamma ND_{13}}^{(1)}}{2mm_\eta} + \frac{g_{\gamma ND_{13}}^{(2)}}{8m^2m_\eta} (\sqrt{s} + m) \right], \quad (\text{A.14})$$

$$A_3 = \frac{eg_{\eta ND_{13}}}{s - M_{D_{13}}^2 + i\Gamma M_{D_{13}}} \left[\frac{g_{\gamma ND_{13}}^{(1)}}{12mm_\eta} (\sqrt{s} - m) \left(2 + \frac{(\sqrt{s} + m)^2}{s} + m \frac{m_\eta^2}{s} \right) \right. \\ \left. + \frac{g_{\gamma ND_{13}}^{(2)}}{48m^2m_\eta} \left(3t - 2m_\eta^2 + (s - m^2) \frac{m + 5\sqrt{s}}{\sqrt{s}} + m \frac{m_\eta^2}{\sqrt{s}} \right) \right], \quad (\text{A.15})$$

$$A_4 = \frac{eg_{\eta ND_{13}}}{s - M_{D_{13}}^2 + i\Gamma M_{D_{13}}} \left[\frac{g_{\gamma ND_{13}}^{(1)}}{12mm_\eta} (\sqrt{s} - m) \left(-4 + \frac{(\sqrt{s} + m)^2}{s} + m \frac{m_\eta^2}{s} \right) \right. \\ \left. + \frac{g_{\gamma ND_{13}}^{(2)}}{48m^2m_\eta} \left(3t - 2m_\eta^2 + (s - m^2) \frac{m - \sqrt{s}}{\sqrt{s}} + m \frac{m_\eta^2}{\sqrt{s}} \right) \right]. \quad (\text{A.16})$$

REFERENCES

- [1] B. Krusche et al., Phys. Rev. Lett. **74** (1995) 3736
- [2] M. Benmerrouche, N.C. Mukhopadhyay, J.F. Zhang, Phys. Rev. D **51** (1995) 3237
- [3] Ch. Sauermann, B.L. Friman, W. Nörenberg, Phys. Lett. **B341** (1995) 261; GSI-Preprint-97-03, nucl-th/9701022
- [4] E. Breitmoser, H. Arenhövel, Nucl. Phys. **A612** (1997) 321
- [5] R.C. Carrasco, Phys. Rev. C **48** (1993) 2333
- [6] TAPS-Experiment at MAMI (1996) (Proposal A2/12-93, Spokesperson: B. Krusche)
- [7] C. Bennhold, H. Tanabe, Nucl. Phys. **A530** (1991) 625
- [8] C. Bennhold, Phys. Rev. C **39** (1989) 1944
- [9] J.D. Bjorken, S.D. Drell, Relativistic Quantum Mechanics (McGraw-Hill, New York, 1964)
- [10] G.F. Chew, M.L. Goldberger, F.E. Low, Y. Nambu, Phys. Rev. **106** (1957) 1345
- [11] L. Tiator, C. Bennhold, S.S. Kamalov, Nucl. Phys. **A580** (1994) 455
- [12] M. Kirchbach, L. Tiator, Nucl. Phys. **A604** (1996) 385
- [13] O. Dumbrajs, R. Koch, H. Pilkuhn, G.C. Oades, H. Behrens, J.J. De Swart, P. Kroll, Nucl. Phys. **B216** (1983) 277
- [14] S.I. Dolinsky et al., Z. Phys. C **42** (1989) 511
- [15] Review of Particle Properties, Phys. Rev. D **54** (1996) 1
- [16] A.I. Fix, V.A. Tryasuchev, Yad. Fiz. **60** (1997) 41 (Phys. Atom. Nucl. **60** (1997) 35)
- [17] H.T. Williams, Phys. Rev. C **31** 2297 (1985)
- [18] R.A. Adelseck, C. Bennhold, L.E. Wright, Phys. Rev. C **32** 1681 (1985)

- [19] Yu.N. Eldyshev, V.N. Lukyanov, Yu.S. Pol, *Yad. Fiz.* **16** (1972) 506 (*Sov. J. Nucl. Phys.* **16** (1973) 282)
- [20] A.A. Chumbalov, R.A. Eramzhyan, S.S. Kamalov, *Z. Phys. A* **328** (1987) 195
- [21] H.S. Sherif, M.S. Abdelmonem, R.S. Sloboda, *Phys. Rev. C* **27** (1983) 2759
- [22] N. Bianchi et al., *Phys. Lett. B* **299** (1993) 219
M. Anghinolfi et al., *Phys. Rev. C* **47** (1993) R922
- [23] B. Krusche, Proceedings of Workshop on Hadrons in Nuclear Matter, Hirschegg, Austria,
eds. H. Feldmeier and W. Nörenberg (GSI, Darmstadt 1995)
- [24] W.M. Alberico, G. Gervino, A. Lavagno, *Phys. Lett. B* **321** (1994) 177
- [25] J. Piekarewicz, A.J. Sarty, M. Benmerrouche, preprint, nucl-th/9701019
- [26] L. Tiator, A.K. Rej, D. Drechsel, *Nucl. Phys. A* **333** (1980) 343
- [27] P. Söding et al., *Phys. Lett. B* **39** (1972) 1
- [28] I. Blomqvist, J.M. Laget, *Nucl. Phys. A* **280** (1977) 405

TABLES

TABLE I. Electromagnetic and hadronic vertices of the elementary $\gamma N \rightarrow \eta N$ model. The symbols e_N and κ_N denote the charge and the anomalous magnetic moment of the nucleon, respectively ($e_p = 1$, $e_n = 0$, and $\kappa_p = 1.79$, $\kappa_n = -1.91$). For the ηNN and ηNN^* vertices only ps coupling is considered.

γNN	$-ee_N\gamma \cdot \varepsilon + i\frac{e\kappa_N}{2m}\sigma_{\mu\nu}k^\mu\varepsilon^\nu$
ηNN	$-ig_{\eta NN}\gamma_5$
$V\eta\gamma$	$\frac{e\lambda}{m_\eta}\varepsilon_{\mu\nu\lambda\sigma}k^\nu\varepsilon^\lambda(p' - p)^\sigma$
VNN	$-g_{VNN}^v\gamma_\mu - i\frac{g_{VNN}^t}{2m}\sigma_{\mu\nu}(p' - p)^\nu$
γNS_{11}	$ie\frac{g_{\gamma\eta S_{11}}}{M_{S_{11}} + m}\gamma_5\sigma_{\mu\nu}k^\mu\varepsilon^\nu$
ηNS_{11}	$-ig_{\eta NS_{11}}$
γND_{13}	$eg_{\gamma ND_{13}}^{(1)}\frac{k_\mu\gamma\cdot\varepsilon - \varepsilon_\mu\gamma\cdot k}{2m} + eg_{\gamma ND_{13}}^{(2)}\frac{\varepsilon_\mu k\cdot p - k_\mu\varepsilon\cdot p}{4m^2}$
ηND_{13}	$-i\frac{g_{\eta ND_{13}}}{m_\eta}\gamma_5q_\mu$

TABLE II. Propagators used in the present calculation. The symbols M , Γ and p_μ denote mass, width and four-momentum of the particle.

spin 1/2	$\frac{\gamma\cdot p + M}{p^2 - M^2 + iM\Gamma}$
spin 1	$\frac{1}{p^2 - M^2} \left[-g_{\mu\nu} + \frac{p_\mu p_\nu}{M^2} \right]$
spin 3/2	$\frac{\gamma\cdot p + \sqrt{s}}{p^2 - M^2 + iM\Gamma} \left[g_{\mu\nu} - \frac{\gamma_\mu\gamma_\nu}{3} - \frac{2}{3}\frac{p_\mu p_\nu}{s} - \frac{\gamma_\mu p_\nu - \gamma_\nu p_\mu}{3\sqrt{s}} \right]$

TABLE III. Coupling constants of the vector mesons.

Vector meson	Mass [MeV]	$(g_{VNN}^v)^2/4\pi$	$(g_{VNN}^t)^2/4\pi$	λ_V
ρ	770	0.55 ± 0.06	20.5 ± 2.1	1.06 ± 0.15
ω	782	8.1 ± 1.5	0.2 ± 0.5	0.31 ± 0.06

TABLE IV. Parameters of the baryon resonances considered in this work. The values for the $D_{13}(1520)$ resonance are taken from the PDG 1996 listings [15], while those for the $S_{11}(1535)$ are obtained by fitting the experimental total cross section data [1]. The helicity couplings A_λ^N are given in units of $10^{-3}\text{GeV}^{-1/2}$.

	$S_{11}(1535)$	$D_{13}(1520)$
Mass [MeV]	1535	1515 – 1530 (1520)
Γ [MeV]	160	110 – 135 (120)
$\Gamma_{\eta N}$ [MeV]	80	0.12
$A_{1/2}^p$	104	-24 ± 9
$A_{1/2}^n$	-88	-59 ± 9
$A_{3/2}^p$		166 ± 5
$A_{3/2}^n$		-139 ± 11

TABLE V. Parameters of the ${}^4\text{He}$ wave function from [21].

j	1	2	3	4	5
a_j [fm $^{-1}$]	1.305	-5.222	7.832	-5.222	1.305
β_j [fm $^{-1}$]	0.0	1.42	2.84	4.26	5.68

FIGURES

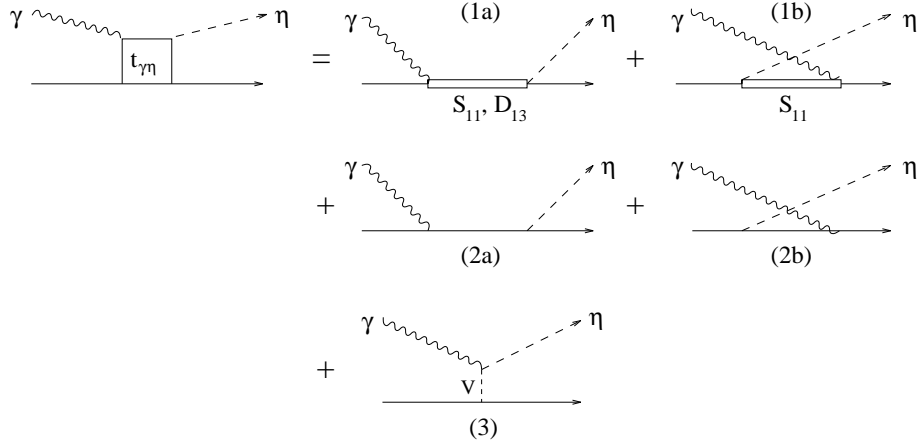


FIG. 1. Diagrams of all contributions to the elementary amplitude: S_{11} and D_{13} resonances in s - (1a) and S_{11} resonance in u -channel (1b), nucleon pole terms in s - (2a) and u -channel (2b), and t -channel vector meson (V) exchange (3).

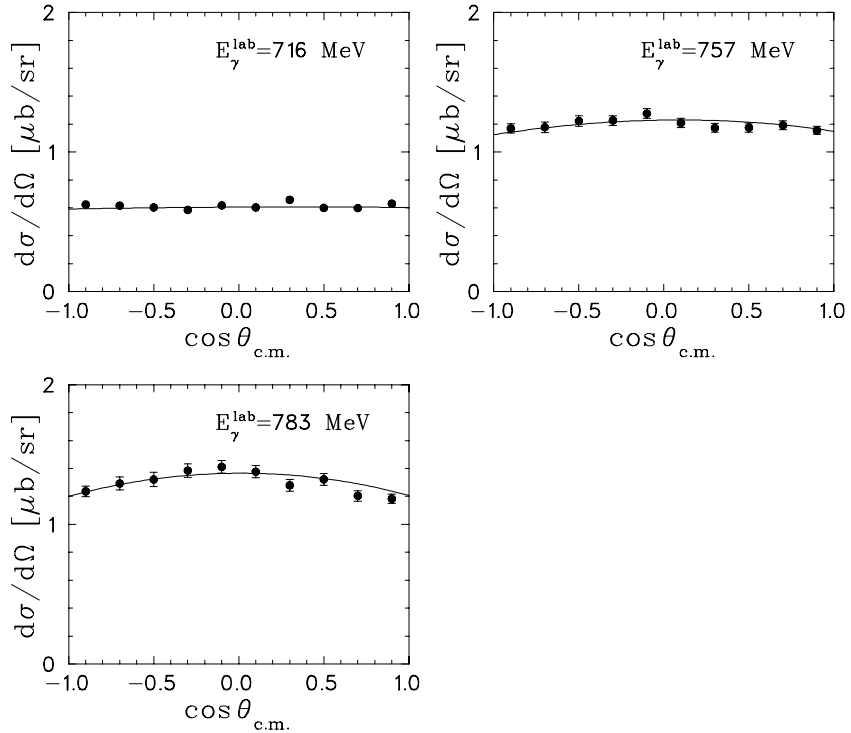


FIG. 2. Comparison of the elementary model for $\gamma p \rightarrow \eta p$ with the Mainz data [1]. The curves were obtained by fitting the $S_{11}(1535)$ parameters.

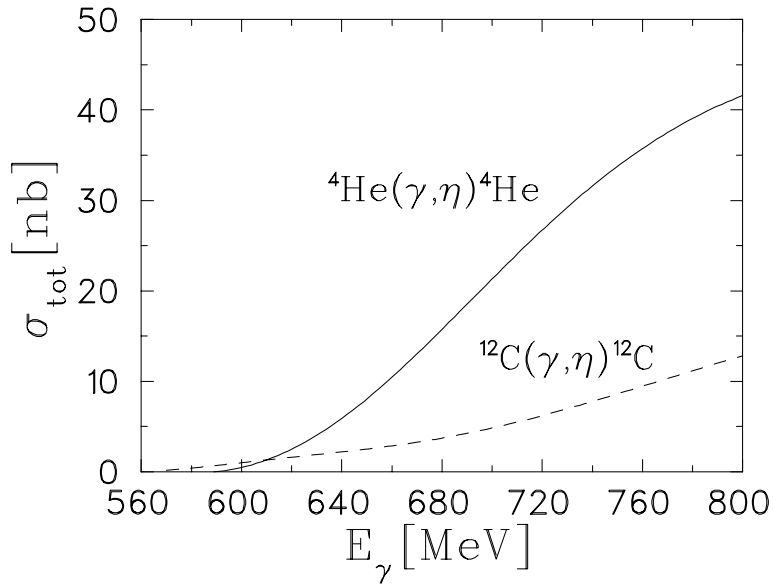


FIG. 3. Total cross section for coherent η -photoproduction on ^4He and ^{12}C .

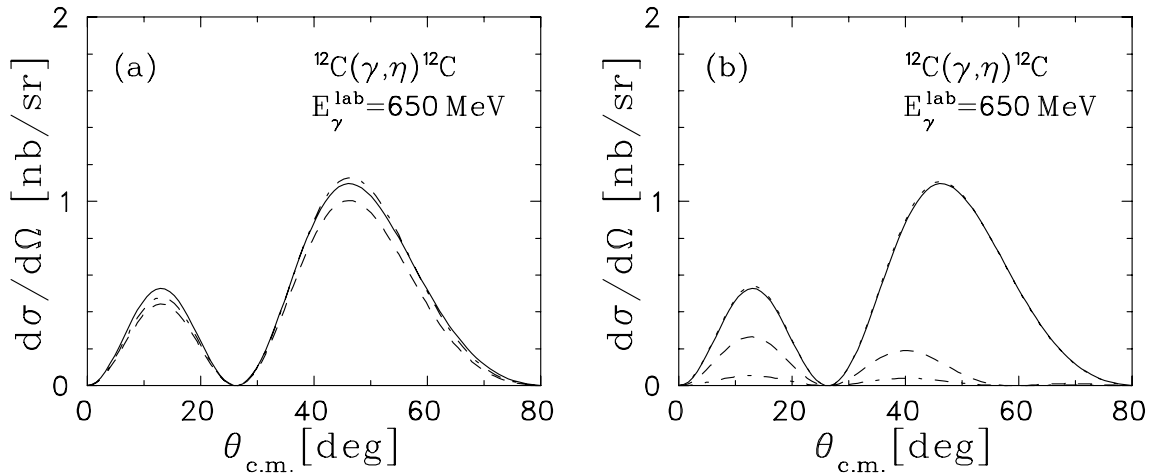


FIG. 4. Differential cross section for $^{12}\text{C}(\gamma, \eta)^{12}\text{C}$. The curves show the contributions from different terms included in the elementary $\gamma N \rightarrow \eta N$ model: (a) full calculation (solid), ω exchange only (dashed), without nucleon pole terms (dash-dotted); (b) full calculation (solid), without $S_{11}(1535)$ (dotted), only $D_{13}(1520)$ with free width Γ (dashed) and with medium modified width Γ^* (dash-dotted).

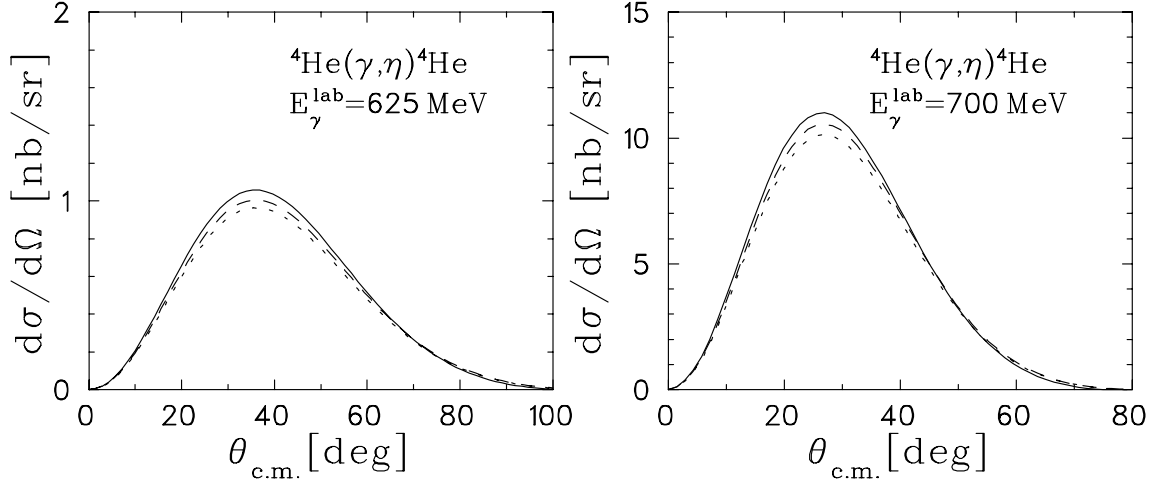


FIG. 5. Differential cross section for the reaction ${}^4\text{He}(\gamma, \eta){}^4\text{He}$ calculated with inclusion of Fermi motion and by taking as invariant energy of the γN subsystem $W_{\gamma N}^{(1)}$ (dashed curves) and $W_{\gamma N}^{(2)}$ (dotted curves). The solid curves are the result of the factorization approximation (25) with on-shell amplitude.

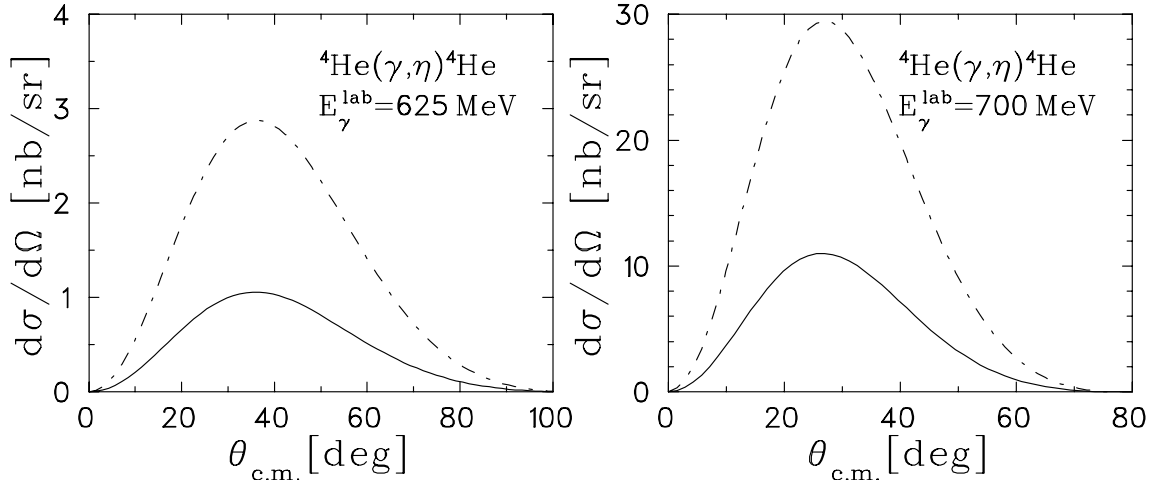


FIG. 6. Influence of the ω -nucleon coupling constant on the differential cross section for ${}^4\text{He}(\gamma, \eta){}^4\text{He}$. Full curve shows the cross section calculated with $g_{\omega NN}^v = 10.3$, and the dash-dotted curve for $g_{\omega NN}^v = 17.5$ from Ref. [28].

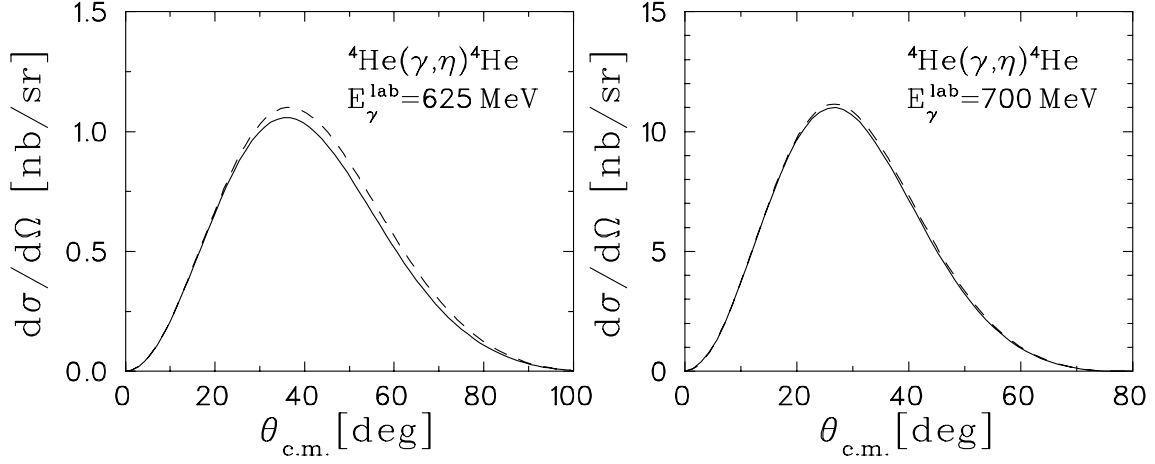


FIG. 7. Comparison of ${}^4\text{He}(\gamma, \eta){}^4\text{He}$ cross sections calculated in the c.m. frame (full) and in the lab frame (dashed) for two photon energies.

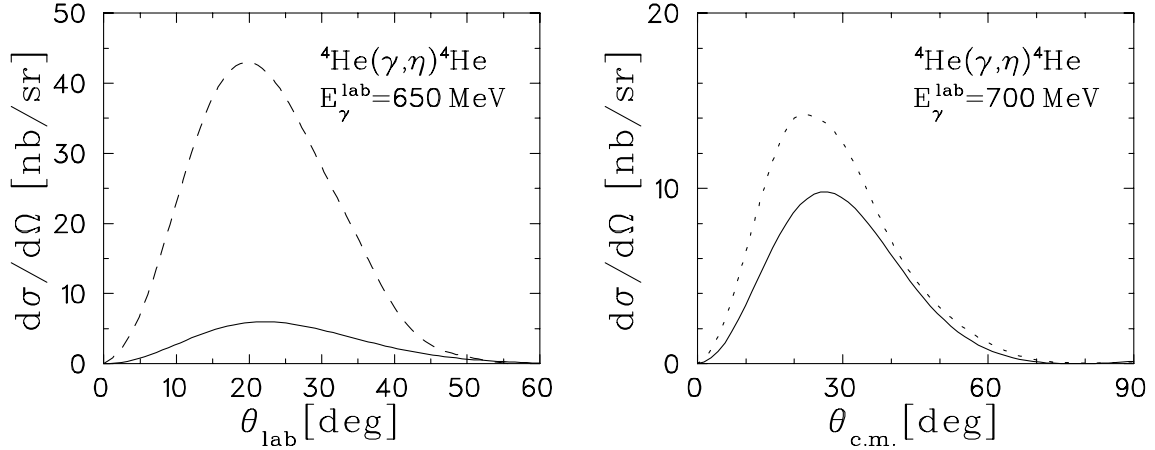


FIG. 8. Comparison of the angular distributions for ${}^4\text{He}(\gamma, \eta){}^4\text{He}$ obtained in the present work (full curves) with the calculations of Ref. [7] (left: dashed) and Ref. [11] (right: dotted).

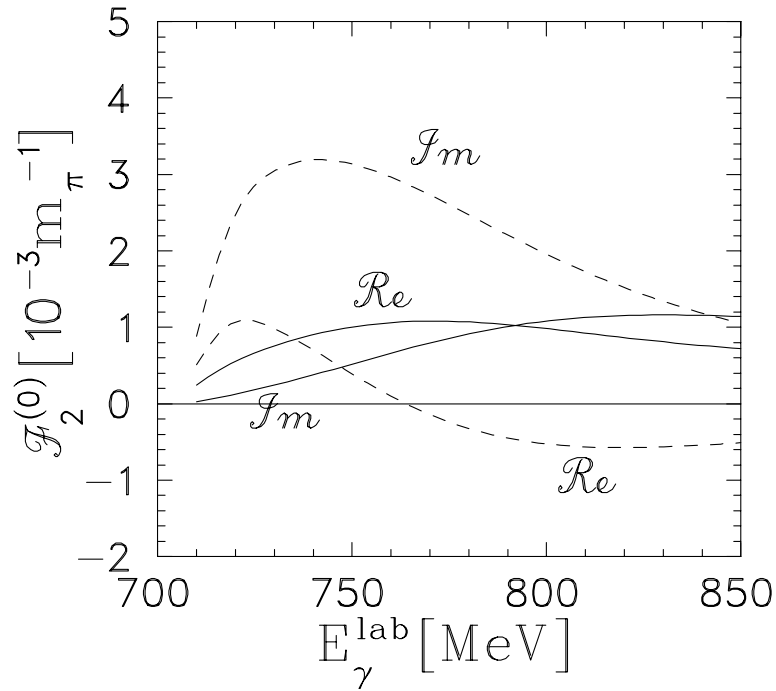


FIG. 9. Comparison of the real and imaginary parts of the CGLN isoscalar amplitude $\mathcal{F}_2^{(0)}(W, \theta)$ for $\theta = 30^\circ$ as predicted in Ref. [7] (dashed) and by our model (solid).